

## Heteroclinic Ratchets in Networks of Coupled Oscillators

Özkan Karabacak · Peter Ashwin

Received: 25 November 2008 / Accepted: 18 July 2009  
© Springer Science+Business Media, LLC 2009

**Abstract** We analyze an example system of four coupled phase oscillators and discover a novel phenomenon that we call a “heteroclinic ratchet”; a particular type of robust heteroclinic network on a torus where connections wind in only one direction. The coupling structure has only one symmetry, but there are a number of invariant subspaces and degenerate bifurcations forced by the coupling structure, and we investigate these. We show that the system can have a robust attracting heteroclinic network that responds to a specific detuning  $\Delta$  between certain pairs of oscillators by a breaking of phase locking for arbitrary  $\Delta > 0$  but not for  $\Delta \leq 0$ . Similarly, arbitrary small noise results in asymmetric desynchronization of certain pairs of oscillators, where particular oscillators have always larger frequency after the loss of synchronization. We call this heteroclinic network a *heteroclinic ratchet* because of its resemblance to a mechanical ratchet in terms of its dynamical consequences. We show that the existence of heteroclinic ratchets does not depend on symmetry or number of oscillators but depends on the specific connection structure of the coupled system.

**Keywords** Synchronization · Coupled oscillators · Heteroclinic ratchet · Asymmetric desynchronization · Synchrony-breaking bifurcation

**Mathematics Subject Classification (2000)** 34C15 · 34C37

---

Communicated by P. Holmes.

Ö. Karabacak (✉) · P. Ashwin  
Mathematics Research Institute, School of Engineering, Computing and Mathematics, University of Exeter, Exeter EX4 4QF, UK  
e-mail: [ozkan2917@yahoo.com](mailto:ozkan2917@yahoo.com)

## 1 Introduction

Coupled phase oscillators arise as simplified models for coupled limit cycle oscillators in case of weak coupling (Strogatz 2000). They have been receiving an increasing interest not only because of their various application areas such as electrochemical oscillators (Zhai et al. 2005; Kiss et al. 2007) and neural systems (Rabinovich et al. 2006b), but also because they present analytically tractable models to understand various kinds of dynamical phenomena (Kuramoto 1984; Hansel et al. 1993; Kori and Kuramoto 2001). These include complete phase synchronization, partial synchronization due to the existence of stable synchronized clusters, and slow switching between unstable clusters. The last phenomenon takes place if there is an attractor containing unstable cluster states which are connected to each other by heteroclinic connections and thus form a heteroclinic network in state space.

Heteroclinic networks (or heteroclinic cycles in particular) are used to explain slow switching behavior of physical systems where a system stays near a dynamically unstable equilibrium or periodic orbit for a long period, then changes its state to another stationary state relatively fast, and repeats this process for another or same stationary state. Despite the fact that heteroclinic networks are not structurally stable, they can be robust if the system considered is constrained by some conditions, such as symmetry (Krupa 1997; Golubitsky and Stewart 2002). This is due to the existence of invariant subspaces on which heteroclinic connections between saddle equilibria can exist robustly.

This robust behavior was first observed in examples of rotating convection and explained by the existence of robust heteroclinic cycle in Busse and Clever (1979) and Guckenheimer and Holmes (1988). Heteroclinic networks are used to explain slow switching phenomenon in different areas such as population dynamics (Hofbauer and Sigmund 1998), electrochemical oscillators (Kiss et al. 2007; Zhai et al. 2005), and neural systems (Rabinovich et al. 2006a, 2006b). They also may have some applications in computational engineering as some recent works (Ashwin and Borresen 2004, 2005; Ashwin et al. 2007) suggest. Especially in complex neural systems, the use of heteroclinic networks is quite promising since this means that one can model persistent transient behavior (Rabinovich et al. 2006b).

In case of full permutation symmetry (all-to-all coupling), a system of  $N$  coupled oscillators can admit robust heteroclinic networks for  $N = 4$  or greater (Ashwin et al. 2008; Ashwin and Borresen 2005). It is important to note that due to the symmetry these heteroclinic networks cannot have arbitrary forms. On the other hand, symmetry is not necessary for robust heteroclinic networks to exist. For example, in Aguiar et al. (2009) it is shown that robust heteroclinic cycles can exist for coupled cell systems with nonsymmetric coupling structure. In this work, we study a coupled phase oscillator system for which robust heteroclinic networks appear as a result of the coupling structure rather than the symmetry of the coupling. This gives rise to heteroclinic networks with some properties that are not seen for symmetric system.

In this paper, we present a new type of heteroclinic network that we call a *heteroclinic ratchet* as it resembles a mechanical ratchet, a device that allows rotary motion on applying a torque in one direction but not in the opposite direction. A *heteroclinic ratchet* on an  $N$ -torus contains heteroclinic cycles winding in some directions but no

other heteroclinic cycles winding in the opposite directions. We show that, for coupled phase oscillators, this type of heteroclinic network can exist as an attractor in phase space resulting in asymmetric desynchronization of certain pairs of oscillators. In other words, oscillators with natural frequencies  $\omega_1$  and  $\omega_2$  break synchrony for  $\Delta = \omega_1 - \omega_2 > 0$  but not for  $\Delta < 0$ . Similarly, when  $\omega_1 = \omega_2$ , arbitrary small noise results in a break of synchrony such that after the desynchronization the observed frequencies  $\Omega_1$  and  $\Omega_2$  satisfy  $\Omega_1 > \Omega_2$ . To the best of our knowledge, this *asymmetric desynchronization* (or *ratcheting*) phenomenon is observed and examined here for the first time. We note that ratcheting cannot take place in all-to-all coupled systems, since the permutation symmetry enforces the system to have desynchronization of a synchronized pair of oscillators in both ways. We will show that the existence of heteroclinic ratchets for a coupled phase oscillator system is mainly related to the coupling structure and does not depend on the symmetry of the system or the number of oscillators.

The main model for coupled phase oscillators is the Kuramoto model of  $N$  oscillators where each oscillator is coupled to all the others by a specific  $2\pi$ -periodic coupling function (Kuramoto 1984). We consider the same model with a specific connection structure and using a more general coupling function  $g(x)$ . Each oscillator has dynamics given by

$$\dot{\theta}_i = \omega_i + \frac{K}{N} \sum_{j=1}^N c_{ij} g(\theta_i - \theta_j). \quad (1)$$

Here  $\dot{\theta}_i \in \mathbb{T} = [0, 2\pi)$ , and  $\omega_i$  is the natural frequency of the oscillator  $i$ . The connection matrix  $\{c_{ij}\}$  represents the coupling between oscillators.  $c_{ij} = 1$  if the oscillator  $i$  receives an input from the oscillator  $j$  and  $c_{ij} = 0$  otherwise. The coupling function  $g$  is a  $2\pi$ -periodic function. For weakly coupled oscillators, it is well known that (1) will have a  $\mathbb{T}^1$  phase-shift symmetry, that is, the dynamics of (1) are invariant under the phase shift

$$(\theta_1, \theta_2, \dots, \theta_N) \mapsto (\theta_1 + \epsilon, \theta_2 + \epsilon, \dots, \theta_N + \epsilon)$$

for any  $\epsilon \in \mathbb{T}$ . We will initially consider identical oscillators, that is,

$$\omega_i = \omega, \quad i = 1, \dots, N, \quad (2)$$

before discussing at a later stage the effect of detuning where the oscillators can have different natural frequencies. Because the coupling function  $g$  is  $2\pi$ -periodic, it is natural to consider a Fourier series expansion

$$g(x) = \sum_{k=1}^{\infty} r_k \sin(kx + \alpha_k), \quad (3)$$

where  $r_k$  must converge to zero fast enough and  $\alpha_k$ 's are arbitrary. Several truncated cases of the general case (3) have been considered in the literature:

- Setting  $r_k = 0$  for  $k = 2, 3, \dots$  and  $\alpha_1 = 0$  gives the Kuramoto model, which exhibits frequency synchronization and clustering phenomena (Kuramoto 1984).

- Setting  $r_k = 0$  for  $k = 2, 3, \dots$  but leaving arbitrary  $\alpha_1$  gives the Kuramoto–Sakaguchi model (Sakaguchi and Kuramoto 1986) with essentially the same dynamics as the Kuramoto model.
- Setting  $r_k = 0$  for  $k = 3, 4, \dots$  and  $\alpha_2 = 0$  gives the model of Hansel et al. (1993). They showed that one can observe new phenomena not present in the above cases. For example, taking

$$r_1 = -1, \quad r_2 = 0.25, \quad \alpha_1 = 1.25$$

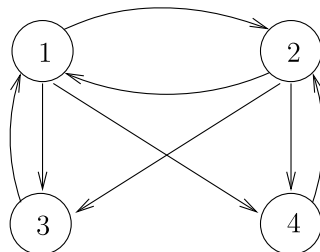
and setting all other parameters to zero, they show that one can observe slow switching phenomenon as a result of the presence of an asymptotically stable robust heteroclinic cycle connecting a pair of saddles.

We investigate a particular coupled 4-cell system that admits a robust heteroclinic ratchet as an attractor only in the presence of a third harmonic in the coupling function, i.e., we will require  $r_3 \neq 0$ . Note that, without loss of generality, we also set  $K = N$  and  $r_1 = -1$  by a scaling of time.

The main coupling structure considered in this work (see Fig. 1) arises as an inflation of the all-to-all coupled 3-cell network. An inflation of a network is obtained by replacing one cell, say  $c$ , by two identical cells, say  $c_1$  and  $c_2$ , in such a way that the synchrony subspace  $\{x_{c_1} = x_{c_2}\}$ , where  $x_{c_i}$  denotes the state of the cell  $c_i$ , is invariant under the dynamics of the new, larger network, and the dynamics of the smaller network are still present within this invariant subspace (see Aguiar et al. 2009 for a mathematical definition). Hence, the network in Fig. 1 admits an  $S_3$ -symmetric quotient network (a smaller network that governs the dynamics on an invariant synchrony subspace), and there may exist symmetry-broken branches of solutions for the coupled systems associated to this network (Aguiar et al. 2007). This is a direct result of the Equivariant Branching Lemma (Golubitsky and Stewart 2002). We will show that for a coupled oscillator system with the coupling structure in Fig. 1, such a synchrony-breaking bifurcation includes two extra pitchfork branches as a result of the  $\mathbb{T}^1$  phase-shift symmetry. These correspond to the saddle cluster states which may form heteroclinic ratchets for some parameter regions.

This work consists of three parts. In Sect. 2, we will analyze the dynamics of the coupled cell system of four phase oscillators and find the invariant subspaces where robust heteroclinic networks can exist. Theorem 1 characterizes a synchrony-breaking bifurcation in such systems. In Sect. 3, we consider a particular coupling function and explain the emergence of a heteroclinic ratchet connecting two pitchfork

**Fig. 1** A 4-cell network: this gives coupled systems of the form (4). Observe that the network has a single symmetry given by the permutation (12)(34)



branches given in Theorem 1. Finally, in Sect. 4, we discuss dynamical consequences of the heteroclinic ratchet considering the influence of noise and detuning of natural frequencies and explore the possible extensions of the 4-cell system to nonsymmetric and higher-dimensional systems.

## 2 An Example of Four Coupled Oscillators

In this section, we consider four oscillators coupled by a connection structure shown in Fig. 1. More specifically, the system we consider is

$$\begin{aligned}\dot{\theta}_1 &= \omega_1 + f(\theta_1; \theta_2, \theta_3), \\ \dot{\theta}_2 &= \omega_2 + f(\theta_2; \theta_1, \theta_4), \\ \dot{\theta}_3 &= \omega_3 + f(\theta_3; \theta_1, \theta_2), \\ \dot{\theta}_4 &= \omega_4 + f(\theta_4; \theta_1, \theta_2).\end{aligned}\tag{4}$$

We first assume identical oscillators, that is,

$$\omega = \omega_1 = \cdots = \omega_4.\tag{5}$$

Oscillators with different natural frequencies will be considered in Sect. 4. We assume that the inputs to each cell are indistinguishable, i.e.,

$$f(x; y, z) = f(x; z, y) \quad \text{for all } x, y, z \in \mathbb{T}.\tag{6}$$

We will also assume the presence of the phase-shift symmetry

$$f(x + \epsilon; y + \epsilon, z + \epsilon) = f(x; y, z) \quad \text{for all } x, y, z, \epsilon \in \mathbb{T}.\tag{7}$$

This  $\mathbb{T}^1$  symmetry arises, for example, in weakly coupled limit cycle oscillators via averaging (Ashwin and Swift 1992). Note that, for the present section, the form of coupling we assume will be more general than (1).

In the following, we discuss the invariant subspaces of (4) and give a result about the solution branches on invariant subspaces that emanate at bifurcation from a fully synchronized solution.

### 2.1 Invariant Subspaces

The network in Fig. 1 has a symmetry that we characterize as follows. Let  $\Gamma$  be the  $S_2$ -action on  $\mathbb{T}^4$  generated by

$$\sigma: (\theta_1, \theta_2, \theta_3, \theta_4) \rightarrow (\theta_2, \theta_1, \theta_4, \theta_3).$$

The symmetry of the network implies that the system (4) is  $\Gamma$ -equivariant and the fixed point subspace of  $\Gamma$ , that is,

$$\text{Fix}(\Gamma) = \{x \in \mathbb{T}^4 \mid \sigma x = x \text{ for all } \sigma \in \Gamma\}$$

**Table 1** Invariant subspaces forced by the coupling structure in Fig. 1 for the system (4)

Dimensions	Invariant Subspaces
4	$V_4 = \mathbb{T}^4$
3	$V_3^s = \{\theta \in \mathbb{T}^4 \mid \theta_3 = \theta_4\}$
3	$V_3^1 = \{\theta \in \mathbb{T}^4 \mid \theta_2 = \theta_4\}$
3	$V_3^2 = \{\theta \in \mathbb{T}^4 \mid \theta_1 = \theta_3\}$
2	$V_2 = \{\theta \in \mathbb{T}^4 \mid \theta_1 = \theta_3, \theta_2 = \theta_4\}$
2	$V_2^{s1} = \{\theta \in \mathbb{T}^4 \mid \theta_2 = \theta_3 = \theta_4\}$
2	$V_2^{s2} = \{\theta \in \mathbb{T}^4 \mid \theta_1 = \theta_3 = \theta_4\}$
2	$V_2^{s3} = \{\theta \in \mathbb{T}^4 \mid \theta_1 = \theta_2, \theta_3 = \theta_4\}$
1	$V_1 = \{\theta \in \mathbb{T}^4 \mid \theta_1 = \theta_2 = \theta_3 = \theta_4\}$

is invariant under the dynamics of (4). On the other hand, there are many other invariant subspaces of which not all appear because of the symmetries of the network but because of the groupoid structure of the input sets of cells (see Golubitsky and Stewart 2006 for groupoid formalism).

These invariant subspaces can be obtained using the balanced coloring method. A coloring of cells, that is, a partition of the set of all cells into a number of groups or colors is called *balanced* if each pair of cells with the same color receive the same number of inputs from the cells with any given color. Each balanced coloring gives rise to an invariant subspace where the states of cells with the same color are equal. Moreover, each balanced coloring corresponds to a quotient network which gives the dynamics reduced to the corresponding invariant subspace.

For the system (4), the invariant subspaces obtained by the balanced coloring method are listed in Table 1. The subscripts indicate the dimensions of the invariant subspaces, and the superscript  $s$  labels the fixed point subspaces related to the  $S_3$  symmetry of the quotient network for  $\theta_3 = \theta_4$  (see Table 2). There exists a partial ordering for the set of these subspaces given by containment, that is,

$$V_x \prec V_y \Leftrightarrow V_x \subset V_y.$$

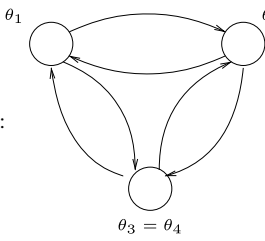
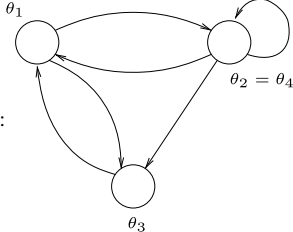
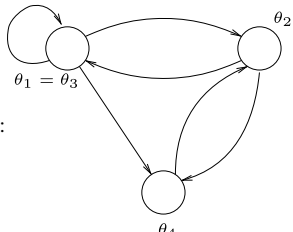
This ordering of invariant subspaces is illustrated in Fig. 2.

Consider the balanced coloring  $\{3, 4\}$ , where only third and forth cells have the same color. The corresponding invariant subspace is  $V_3^s$ , and the quotient network is the  $S_3$ -symmetric all-to-all coupled 3-cell network (see Table 2). Necessarily all the fixed point subspaces of this 3-cell quotient lift to some invariant subspaces of the 4-cell system, and these are labeled by the superscript  $s$ . Note that  $V_2^{s3}$  is the only one of these that arises from the symmetry of the system (4) ( $V_2^{s3} = \text{Fix}(\Gamma)$ ), but there are some pairs of subspaces for which one subspace is related to the other by the symmetry of the system, namely  $\sigma(V_2^{s2}) = V_2^{s1}$  and  $\sigma(V_3^2) = V_3^1$ . As a result, the quotient networks corresponding the subspaces  $V_3^1$  and  $V_3^2$  are also symmetrically related (see Table 2).

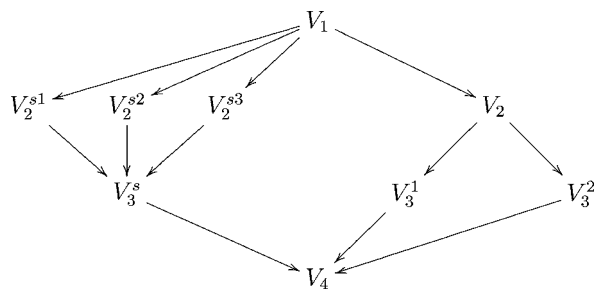
Exploiting the phase-shift symmetry (7), the four-dimensional system (4) and (5) can be reduced to a three-dimensional one by defining new variables

$$(\phi_1, \phi_2, \phi_3) := (\theta_1 - \theta_3, \theta_2 - \theta_4, \theta_3 - \theta_4)$$

**Table 2** Quotient networks for the three-dimensional invariant subspaces  $V_3^s$ ,  $V_3^1$ , and  $V_3^2$  of the 4-cell system (4)

Balanced Colorings	Invariant Subspaces	Quotient Networks
{3, 4}	$V_3^s$	$N_1 :$ 
{2, 4}	$V_3^1$	$N_2 :$ 
{1, 3}	$V_3^2$	$N_3 :$ 

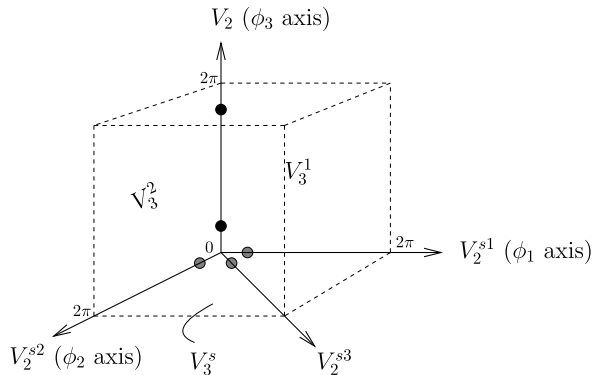
**Fig. 2** Containment of the invariant subspaces given in Table 1.  $V_x \rightarrow V_y$  means  $V_x \subset V_y$ . The subscripts indicate the dimensions of the invariant subspaces, and the superscript  $s$  labels the fixed point subspaces related to the  $S_3$  symmetry of the quotient network for  $\theta_3 = \theta_4$



so that

$$\begin{aligned}
 \dot{\phi}_1 &= f(\phi_1; \phi_2 - \phi_3, 0) - f(0; \phi_1, \phi_2 - \phi_3), \\
 \dot{\phi}_2 &= f(\phi_2; \phi_1 + \phi_3, 0) - f(0; \phi_1 + \phi_3, \phi_2), \\
 \dot{\phi}_3 &= f(\phi_3; \phi_1 + \phi_3, \phi_2) - f(0; \phi_1 + \phi_3, \phi_2).
 \end{aligned}
 \tag{8}$$

**Fig. 3** Invariant subspaces given in Table 1 projected onto  $\mathbb{T}^3$  (represented by a  $2\pi$ -cube in  $\mathbb{R}^3$ ) and the synchrony-broken branches given in Theorem 1. Subscripts indicate the subspace dimensions on  $\mathbb{T}^4$ . The bifurcating branches of equilibria given in Theorem 1 are represented by *disks* filled by black and gray colors for pitchfork and transcritical branches, respectively



The symmetry of the system (4) has implications for this system. Let  $\tilde{I}$  be the  $S_2$ -action on  $\mathbb{T}^3$  generated by

$$\rho : (\phi_1, \phi_2, \phi_3) \rightarrow (\phi_2, \phi_1, -\phi_3)_{\text{mod } 2\pi}. \quad (9)$$

Then the system (8) is  $\tilde{I}$  equivariant. In this case the fixed point subspaces are the lines  $\{\phi \in \mathbb{T}^3 \mid \phi_1 = \phi_2, \phi_3 = 0\}$  and  $\{\phi \in \mathbb{T}^3 \mid \phi_1 = \phi_2, \phi_3 = \pi\}$ . Other invariant subspaces can be obtained projecting the previously found invariant subspaces onto  $\mathbb{T}^3$ . These are illustrated in Fig. 3, where the previous notation for subspaces is used. That is, subscripts indicate dimensions of the subspaces in  $\mathbb{T}^4$ .

## 2.2 Synchrony-breaking bifurcations

For this section, we assume that  $f$  depends on a parameter  $\alpha$ . Hence, we can rewrite (8) as

$$\begin{aligned} \dot{\phi}_1 &= f(\phi_1; \phi_2 - \phi_3, 0; \alpha) - f(0; \phi_1, \phi_2 - \phi_3; \alpha), \\ \dot{\phi}_2 &= f(\phi_2; \phi_1 + \phi_3, 0; \alpha) - f(0; \phi_1 + \phi_3, \phi_2; \alpha), \\ \dot{\phi}_3 &= f(\phi_3; \phi_1 + \phi_3, \phi_2; \alpha) - f(0; \phi_1 + \phi_3, \phi_2; \alpha). \end{aligned} \quad (10)$$

We denote the zero vector by  $\mathbf{0}$  and use  $f(\mathbf{0}, \alpha) = f(0; 0, 0; \alpha)$ .

In Aguiar et al. (2007), it is shown that any coupled cell system that has a connection structure as in Fig. 1 admits an  $S_3$ -transcritical bifurcation on  $V_3^s$  at the origin. More concretely, there exist three transcritical branches of unstable solutions on  $V_2^{s1}$ ,  $V_2^{s2}$ , and  $V_2^{s3}$  simultaneously emanating from the origin if  $f_x(\mathbf{0}, 0) - f_y(\mathbf{0}, 0) = 0$  and some transversality inequalities are satisfied. However, for the coupled phase oscillators of type (4), apart from the connection structure, dynamical properties affect the bifurcation scheme. Now we will show in Theorem 1 how the  $\mathbb{T}^1$  symmetry of  $f$  gives rise to a pitchfork bifurcation on  $V_2$  that takes place simultaneously with the transcritical bifurcations mentioned above. The occurrence of simultaneous branches on invariant lines is not only a consequence of the Equivariant Branching Lemma (Golubitsky and Stewart 2002) but also a result of the connection structure and the property of the individual dynamics, that is, the  $\mathbb{T}^1$  symmetry of  $f$ .



**Table 3** Adjacency matrix of the network in Fig. 1 with eigenvalues and eigenvectors

Adjacency matrix	Eigenvalues and eigenvectors
$A = \begin{pmatrix} 0 & 1 & 1 & 0 \\ 1 & 0 & 0 & 1 \\ 1 & 1 & 0 & 0 \\ 1 & 1 & 0 & 0 \end{pmatrix}$	$\begin{aligned} \mu_1 &= -1, v_1 = (1, -1, 0, 0)^T \\ \mu_2 &= -1, v_2 = (0, -1, 1, 1)^T \\ \mu_3 &= 0, v_3 = (1, -1, 1, -1)^T \\ \mu_4 &= 2, v_4 = (1, 1, 1, 1)^T \end{aligned}$

**Theorem 1** Assume that  $f$  satisfies  $f_x(\mathbf{0}, \alpha^*) = 0$ ,  $f_{x\alpha}(\mathbf{0}, \alpha^*) \neq 0$ ,  $f_{xx}(\mathbf{0}, \alpha^*) \neq f_{yy}(\mathbf{0}, \alpha^*)$ , and  $f_{xxx}(\mathbf{0}, \alpha^*) - 6f_{xyy}(\mathbf{0}, \alpha^*) \neq 0$ . Then there exists a pitchfork bifurcation of the origin of (10) on  $V_2$  at  $\alpha = \alpha^*$  appearing simultaneously with the transcritical bifurcations on  $V_2^{s1}$ ,  $V_2^{s2}$  and  $V_2^{s3}$ .

**Remark 1** A direct consequence of Theorem 1 is that a generic bifurcation of the fully synchronized periodic solution  $(x, x, x, x)$  of (4) will give rise to three branches of periodic solutions of the form

$$\begin{aligned} (x, y, x, x), \\ (y, x, x, x), \\ (x, x, y, y), \end{aligned}$$

and two other branches of the form  $(x, y, x, y)$ , where the first three appear by transcritical bifurcations and the final two via a pitchfork bifurcation.

*Proof* Consider the adjacency matrix  $A$  of the network (see Table 3). The eigenvalues of  $A$  and partial derivatives of  $f$  ( $f_x$ ,  $f_y$ , and  $f_z$ ) at the origin determine the stability of the origin (see Proposition 2 in Aguiar et al. 2007). The eigenvalues of (10) at the origin are

$$\lambda_i = f_x(\mathbf{0}, \alpha) + \mu_i f_y(\mathbf{0}, \alpha), \quad (11)$$

where  $\mu_i$  is an eigenvalue of  $A$ , and  $i = 1, 2, 3$ . The eigenvectors of (10) are the same as the eigenvectors of  $A$  that correspond to its nonzero eigenvalues. It is important to note that the  $\mathbb{T}^1$  phase-shift symmetry of (4) induce a relation between partial derivatives:

$$f_x(u, v, w, \alpha) + f_y(u, v, w, \alpha) + f_z(u, v, w, \alpha) = 0 \quad \forall u, v, w, \alpha \in \mathbb{R}. \quad (12)$$

This can be obtained taking the derivative of (7) with respect to  $\epsilon$ , and (6) implies

$$f_y(u, v, w, \alpha) = f_z(u, w, v, \alpha) \quad \forall u, v, w, \alpha \in \mathbb{R}. \quad (13)$$

Thus, by (12) and (13), there exists a linear relationship between partial derivatives:

$$f_x(\mathbf{0}, \alpha) = -2f_y(\mathbf{0}, \alpha) = -2f_z(\mathbf{0}, \alpha) \quad \forall \alpha \in \mathbb{R}. \quad (14)$$

Similarly, derivatives of (12) and (13) with respect to  $\alpha$  give

$$f_{x\alpha}(\mathbf{0}, \alpha) = -2f_{y\alpha}(\mathbf{0}, \alpha) = -2f_{z\alpha}(\mathbf{0}, \alpha) \quad \forall \alpha \in \mathbb{R}, \quad (15)$$

and derivative of (13) with respect to  $v$  gives

$$f_{yy}(\mathbf{0}, \alpha) = f_{zz}(\mathbf{0}, \alpha) \quad \forall \alpha \in \mathbb{R}. \quad (16)$$

Finally, from the multiple derivatives of (12) and (13) with respect to  $u$ ,  $v$  and  $w$ , one can estimate

$$f_{zzz}(\mathbf{0}, \alpha) = f_{yyy}(\mathbf{0}, \alpha) = (f_{xxx}(\mathbf{0}, \alpha) - 6f_{xyy}(\mathbf{0}, \alpha))/4 \quad \forall \alpha \in \mathbb{R}. \quad (17)$$

Equations (11) and (14) imply that the eigenvalues  $\lambda_i$  become zero simultaneously when  $f_x(\mathbf{0}, \alpha) = 0$ . To see that there exists a pitchfork branch on  $V_2$ , we consider the solutions of type  $(x, x + u, x, x + u)$ . Substituting this into (10) and using (7), one gets  $\dot{u} = F(u) := f(0; 0, -u, \alpha) - f(0; u, 0, \alpha)$ . Thus the assumptions  $f_x(\mathbf{0}, \alpha^*) = 0$ ,  $f_{x\alpha}(\mathbf{0}, \alpha^*) \neq 0$ , and  $f_{xxx}(\mathbf{0}, \alpha^*) - 6f_{xyy}(\mathbf{0}, \alpha^*) \neq 0$  and (14)–(17) imply the pitchfork bifurcation conditions  $(\partial F / \partial u)(\mathbf{0}, \alpha^*) = 0$ ,  $(\partial^2 F / \partial u^2)(\mathbf{0}, \alpha^*) = 0$ ,  $(\partial^2 F / \partial \alpha \partial u)(\mathbf{0}, \alpha^*) \neq 0$ , and  $(\partial^3 F / \partial u^3)(\mathbf{0}, \alpha^*) \neq 0$ . Since these and the condition  $f_{xx}(\mathbf{0}, \alpha^*) \neq f_{yy}(\mathbf{0}, \alpha^*)$  also imply the assumptions of Theorem 1 in Aguiar et al. (2007), there exist simultaneous transcritical bifurcations on  $V_2^{s1}$ ,  $V_2^{s2}$ , and  $V_2^{s3}$ .  $\square$

**Remark 2** The existence of pitchfork branches can also be explained by considering the  $S_2$  interior symmetry of the set of cells  $\{3, 4\}$  in Fig. 1 (see Golubitsky et al. 2004 for the concept of *interior symmetry* and the *interior symmetry branching lemma*). However, this does not imply the simultaneous occurrence of transcritical and pitchfork branches for the system (10).

### 3 Robust Heteroclinic Ratchets for the System of Four Coupled Oscillators

For a vector field  $F : \mathbb{R}^N \rightarrow \mathbb{R}^N$  (or  $\mathbb{T}^N \rightarrow \mathbb{T}^N$ ), a *heteroclinic cycle* consists of a set of saddle equilibria  $\xi_0, \dots, \xi_{m-1}$  and trajectories (connections)  $x_0(t), \dots, x_{m-1}(t)$  such that  $\lim_{t \rightarrow -\infty} x_i(t) = \xi_i$  and  $\lim_{t \rightarrow \infty} x_i(t) = \xi_{i+1 \pmod{m}}$  for  $i = 0, \dots, m-1$ . We call a connected invariant set a *heteroclinic network* if it is a union of heteroclinic cycles.

In the previous section, it is shown that the connection structure of the system (4) induces the existence of invariant subspaces. These subspaces persist under the perturbations that preserve the connection structure. For this reason, as in symmetric systems, one can find robust heteroclinic networks lying on the invariant subspaces of the system (4). By “robust” we mean the persistence under small perturbations that preserve the coupling structure. We will see that for the phase-difference system (8) some unusual heteroclinic networks exist, which are not seen for symmetric systems. We distinguish one type of these heteroclinic networks, which we call a *heteroclinic ratchet* because it includes connections that wind around the torus in one direction only.

**Definition 1** For a system on  $\mathbb{T}^N$ , a heteroclinic network is a *heteroclinic ratchet* if it includes a heteroclinic cycle with nontrivial winding in one direction but no heteroclinic cycles winding in the opposite direction. More precisely, we say that a

heteroclinic cycle  $C \subset \mathbb{T}^N$  parameterized by  $x(s)$  ( $x: [0, 1) \rightarrow \mathbb{T}^N$ ) has *nontrivial winding in some direction* if there is a projection map  $P: \mathbb{R}^N \rightarrow \mathbb{R}$  such that the parameterization  $\bar{x}(s)$  ( $\bar{x}: [0, 1) \rightarrow \mathbb{R}^N$ ) of the lifted heteroclinic cycle  $\bar{C} \subset \mathbb{R}^N$  satisfies  $\lim_{s \rightarrow 1} P(\bar{x}(s)) - P(\bar{x}(0)) = 2k\pi$  for some positive integer  $k$ . A heteroclinic cycle winding in the opposite direction would satisfy the same condition for a negative integer  $k$ .

In this section, we will first explain how a heteroclinic ratchet emerges for the system (8) after a synchrony-breaking bifurcation. Then, we will discuss the stability of the heteroclinic ratchet and exhibit a coupling function  $g$  for which the heteroclinic ratchet is an attractor. Finally, different routes that lead to heteroclinic cycles will be discussed.

### 3.1 Heteroclinic Ratchets for the Four Coupled Oscillators

We consider a particular case of (4), with coupling having the same form as (1):

$$f(x; y, z) = g(x - y) + g(x - z). \quad (18)$$

Using (18), we can write the phase-difference system with identical natural frequencies given in (8) in the form

$$\begin{aligned} \dot{\phi}_1 &= g(\phi_1 + \phi_3 - \phi_2) + g(\phi_1) - g(-\phi_1) - g(\phi_3 - \phi_2), \\ \dot{\phi}_2 &= g(\phi_2 - \phi_3 - \phi_1) + g(\phi_2) - g(-\phi_3 - \phi_1) - g(-\phi_2), \\ \dot{\phi}_3 &= g(-\phi_1) + g(\phi_3 - \phi_2) - g(-\phi_3 - \phi_1) - g(-\phi_2). \end{aligned} \quad (19)$$

We consider the coupling function  $g$  with up to three harmonics:

$$g(x) = -\sin(x + \alpha_1) + r_2 \sin(2x) + r_3 \sin(3x). \quad (20)$$

For this coupling function, there may exist different types of robust heteroclinic networks for different parameter values. We first demonstrate a heteroclinic ratchet that exists for an open set of parameters.

Heteroclinic networks are usually exceptional phenomena, but they can be robust if the associated heteroclinic connections are contained within invariant subspaces (Krupa 1997). For (19) and (20), there are invariant subspaces that are found in the previous section for a more general system (8) (see Fig. 3). For the parameter set

$$(\alpha_1, r_2, r_3) = (1.4, 0.3, -0.1), \quad (21)$$

we identify robust heteroclinic connections between two equilibria on the invariant subspaces  $V_3^1$  and  $V_3^2$ , using the simulation tool XPPAUT (Ermentrout 2002). Note that the symmetry (9) of (8) acts on  $V_2 = V_3^1 \cap V_3^2$  ( $\phi_3$  axis) as  $(0, 0, x) \rightarrow (0, 0, -x) \bmod{2\pi}$ . Therefore, an equilibrium  $p = (0, 0, p_3)$  on  $V_2$  has its symmetric counterpart on  $V_2$  as  $q = \sigma(p) = (0, 0, 2\pi - p_3)$ . These equilibria  $p$  and  $q$  with the connections between them on the invariant planes  $V_3^1$  and  $V_3^2$  form the heteroclinic network in Fig. 4.

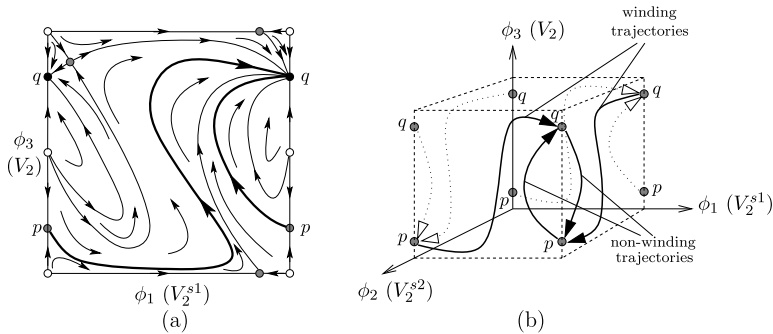


**Fig. 4** Heteroclinic ratchet for the system (19), (20) with the parameter set (21). Sources, saddles, and sinks are indicated by *small disks* filled with white, gray, or black color, respectively. **(a)** Phase portrait on  $V_3^1$  (projected onto  $\mathbb{T}^2$ ). **(b)** The heteroclinic ratchet on  $\mathbb{T}^3$  (represented by a  $2\pi$ -cube in  $\mathbb{R}^3$ )

Recall that the subspaces  $V_3^1$  and  $V_3^2$  are mapped to each other by the symmetry (9). Thus, the presence of a connection from  $p$  to  $q$  on  $V_3^1$  implies the presence of another connection on  $V_3^2$  that connects  $q$  to  $p$ . Therefore, in order to verify the existence of a heteroclinic network in  $\mathbb{T}^3$ , it suffices to identify connections from  $p$  to  $q$  on  $V_3^1$ , as done in Fig. 4a for the parameter set (21). Note that this is a heteroclinic ratchet since it includes phase slips in the directions  $+\phi_1$  and  $+\phi_2$  only (see the winding trajectories in Fig. 4b).

The winding connections of the heteroclinic ratchet are contained in symmetrically related subspaces  $V_3^1$  and  $V_3^2$  (Fig. 3), where the dynamics are governed by the quotient networks  $N_2$  and  $N_3$  illustrated in Table 2. However, neither  $N_2$  nor  $N_3$  has a network symmetry, and this can be related to the existence of the heteroclinic ratchet, since a symmetry in these networks may leave out the possibility for a winding orbit or may result in symmetric connections winding in opposite directions.

### 3.2 Stability of the Heteroclinic Ratchet

A necessary and sufficient condition for stability of a heteroclinic cycle in  $\mathbb{R}^3$  whose connections are included in two-dimensional invariant regions is given in terms of the eigenvalues of equilibria by Melbourne (1989) (for more results on stability of heteroclinic cycles, see Feng and Hu 2003; Krupa and Melbourne 1995). Melbourne proves that eigenvalues  $\lambda^0(\xi_i) < 0$  corresponding to the eigenvectors tangent to the intersection of the invariant regions are irrelevant for the stability of heteroclinic cycles and only the saddle quantities  $\sigma_i = |\lambda^+(\xi_i)/\lambda^-(\xi_i)|$  determine the stability, where  $\xi_i$  is a saddle in the heteroclinic cycle, and  $\lambda^-(\xi_i) < 0$  ( $\lambda^+(\xi_i) > 0$ ) is the eigenvalue at  $\xi_i$  corresponding to the eigenvector on the stable (unstable) manifold of  $\xi_i$  that is not contained in the intersection of the invariant regions. Note that the eigenvalues  $\lambda^0(\xi_i)$  that correspond to the eigenvectors in the intersection of the invariant regions are necessarily negative for robustness (saddle-to-sink connections on invariant regions). Under some generic assumptions, a heteroclinic cycle in  $\mathbb{R}^3$  whose connections are contained in two-dimensional invariant regions is asymptotically stable if  $\prod_i \sigma_i < 1$  and is unstable if  $\prod_i \sigma_i > 1$  (see Appendix in Melbourne 1989).

We denote by  $\lambda^+(p)$  the eigenvalue of  $p$  corresponding to the eigenvector tangent to the unstable manifold of  $p$  in  $V_3^1$  and by  $\lambda^-(p)$  the eigenvalue of  $p$  corresponding to the eigenvector contained in  $V_3^2 \setminus V_2$ . A heteroclinic cycle in Melbourne (1989) is defined as a set of saddle equilibria and their one-dimensional unstable manifolds, and it is assumed that each of these unstable manifolds is contained in a stable manifold of some equilibrium inside the heteroclinic cycle. Therefore, the heteroclinic ratchet in Fig. 4 satisfies this definition. Since in our example the equilibria  $p$  and  $q$  are symmetrically related, it follows from Melbourne (1989) that the heteroclinic ratchet in Fig. 4 is asymptotically stable if  $|\lambda^+(p)/\lambda^-(p)| < 1$  and unstable if  $|\lambda^+(p)/\lambda^-(p)| > 1$ . For the parameter set (21), the equilibrium is at  $p = 1.4432$ . Then,  $\lambda^+(p)$  and  $\lambda^-(p)$  are 0.74 and  $-1.2$  by linearizing (19) at  $p$  (see (29)). This implies the asymptotic stability of the heteroclinic ratchet.

Since the condition for the asymptotic stability is open and the heteroclinic connections are robust, one can find an open set in the parameter space  $\{(\alpha_1, r_2, r_3) \mid 0 \leq r_2, r_3, 0 \leq \alpha_1 < 2\pi\}$ , for which the system (19) admits an asymptotically stable robust heteroclinic ratchet. On the other hand, for the system (19), the robust heteroclinic ratchet connecting a pair of saddles  $p$  and  $q$  on  $V_3^1$  cannot be asymptotically stable if  $r_3 = 0$  (see Appendix). Therefore, the heteroclinic ratchets for the system (19) cannot be asymptotically stable unless the third or higher harmonics of the coupling function  $g$  are taken into account.

### 3.3 Routes to Heteroclinic Ratchets

The equilibria  $p$  and  $q$  in  $V_2 = V_3^1 \cap V_3^2$  bifurcate from the origin via a pitchfork bifurcation simultaneously with other transcritical branches of solutions on  $V_2^{s1}$ ,  $V_2^{s2}$ , and  $V_2^{s3}$ . This synchrony-breaking bifurcation is discussed in Theorem 1. Although we cannot rule out the possibility of the presence of more complex behaviors near this bifurcation, we numerically find the heteroclinic ratchet for the parameter values close to the bifurcation point. This suggests that the bifurcation given in Theorem 1 may be associated with a global bifurcation to a heteroclinic ratchet.

Although the subspace  $V_3^s$  does not include any part of the heteroclinic networks, the dynamics restricted to this subspace, that is, the dynamics of the network  $N_1$  (see Table 2) give rise to another bifurcation to a heteroclinic ratchet as seen in Fig. 5. The detailed bifurcation analysis of the 3-cell all-to-all coupled oscillators with a coupling function having the first two harmonics is given in Ashwin et al. (2008). There, it is stated that apart from the transcritical bifurcation of the origin, there exists a saddle-node bifurcation on invariant lines. This bifurcation should also exist for nonzero  $r_3$  values. In Fig. 5a–c, phase portraits on  $V_3^1$  are illustrated for  $\alpha_1 = 1.2$ ,  $\alpha_1 \cong 1.327$ , and  $\alpha_1 = 1.4$ , respectively, while  $r_2 = 0.3$  and  $r_3 = -0.1$  are fixed. As  $\alpha_1$  increases, a sink and a saddle equilibrium on  $V_2^{s1}$  (see Fig. 5a) collide (Fig. 5b) and disappear by a reverse saddle-node bifurcation giving rise to a winding connection from  $p$  to  $q$  (see Fig. 5c). With this disappearance of the sink on  $V_2^{s1}$  (and on  $V_2^{s2}$  by symmetry), a heteroclinic cycle (see Fig. 5d) that exists for the parameter set

$$(\alpha_1, r_2, r_3) = (1.2, 0.3, -0.1) \quad (22)$$

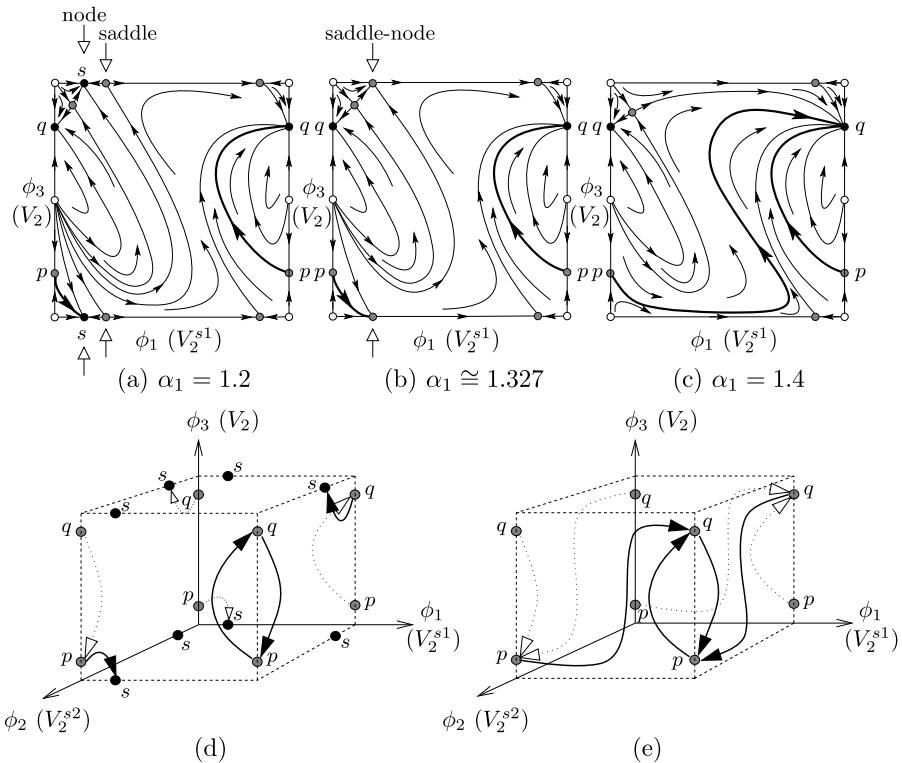


**Fig. 5** Phase portraits for the system (19), (20) on  $V_3^1$  for  $r_2 = 0.3$ ,  $r_3 = -0.1$ , and for different  $\alpha$  parameters demonstrating a bifurcation from a heteroclinic cycle to a heteroclinic ratchet shown in (d) and (e), respectively. As  $\alpha_1$  increases, the reverse saddle-node bifurcation indicated in (a)–(c) takes place resulting in disappearance of the sink  $s$  and therefore changes the structure of the unstable manifold of  $p$ . This gives rise in a global bifurcation from a heteroclinic cycle (d) to a heteroclinic ratchet (e). (For each graph, sources, saddles, and sinks are indicated by *small disks* filled with white, gray, or black color, respectively. The unstable manifolds of  $p$  are shown by *thick lines*)

bifurcates to the heteroclinic ratchet which is observed in the previous section for the parameter set (21) (see Fig. 5e). Therefore, this bifurcation describes another route to heteroclinic ratchets where  $\mathbb{T}^1$  symmetry is not necessary (see Sect. 4.4 for a heteroclinic ratchet in a system without symmetry).

Although the heteroclinic cycle seen for the parameter set (22) satisfies  $|\lambda^+(p)/\lambda^-(p)| = |0.68/-0.7| < 1$ , it is not stable because  $p$  has an unstable manifold which approaches a sink  $s$  outside the heteroclinic ratchet (see Figs. 5a and 5d). This type of heteroclinic cycle is also unusual for symmetric systems. It attracts nearby trajectories with initial states  $\phi(0)$  close to  $p$  and with  $\phi_1(0)$ ,  $\phi_2(0)$  on the left of  $0 \in \mathbb{T}^1$ , whereas other nearby trajectories with initial states  $\phi(0)$  close to  $p$  and with  $\phi_1(0)$  or  $\phi_2(0)$  on the right of  $0 \in \mathbb{T}^1$  converge to the sink  $s$  because of the connection from  $p$  to  $s$  (see Fig. 5d). Therefore, this heteroclinic cycle has a basin with positive measure, so it is a Milnor attractor (Milnor 1985), though not stable.

## 4 Discussion and Dynamical Consequences of the Heteroclinic Ratchet

This paper has so far demonstrated that the system of four coupled oscillators in Fig. 1 with identical natural frequencies  $\omega_i$  can support a robust heteroclinic attractor analogous to a mechanical ratchet. In this section, we consider the response of such an attractor to imperfections in the system. In particular, we consider the effect of setting the detunings

$$\Delta_{ij} = \omega_i - \omega_j$$

to be nonzero, and the effect of adding noise to the system. The frequency locking response to detuning and/or noise is an indicator of the heteroclinic ratchet.

For typical trajectories in terms of the original phases  $\theta_i(t) \in \mathbb{R}$ , one can define the average frequency of the  $i$ th oscillator  $\Omega_i = \lim_{t \rightarrow \infty} \frac{\theta_i(t)}{t}$  and the frequency difference

$$\Omega_{ij} = \lim_{t \rightarrow \infty} \frac{\theta_i(t) - \theta_j(t)}{t}.$$

**Definition 2** We say the  $i$ th and  $j$ th oscillators are *frequency synchronized* on an attractor of the system if all trajectories approaching the attractor satisfy  $\Omega_{ij} = 0$ .

Note that a stronger notion of synchrony is phase synchronization; we say the  $i$ th and  $j$ th oscillators are *phase synchronized* if all trajectories approaching the attractor have  $\theta_i(t) - \theta_j(t)$  bounded in  $t$ . Phase synchronization is a sufficient condition for frequency synchronization, but the converse is not always true as we see below.

### 4.1 Response of the System to Detuning

Note that in the case of identical natural frequencies, the oscillators of the original system are frequency synchronized for all trajectories; this follows because trajectories of the reduced phase-difference system are trapped inside a bounded invariant region, namely the boundary of the  $2\pi$ -cube in Fig. 3, and so they are phase synchronized. As soon as  $\Delta_{ij} \neq 0$  for some  $i, j$ , this may no longer be the case. Here, we choose three independent detuning variables as  $\Delta_{13}$ ,  $\Delta_{24}$ , and  $\Delta_{34}$  so that the natural frequencies can be written as

$$\begin{aligned}\omega_1 &= \omega + \Delta_{13} + \Delta_{34}, \\ \omega_2 &= \omega + \Delta_{24}, \\ \omega_3 &= \omega + \Delta_{34}, \\ \omega_4 &= \omega.\end{aligned}\tag{23}$$

Using (23) instead of (5), phase-difference system (8) can be rewritten as

$$\begin{aligned}\dot{\phi}_1 &= \Delta_{13} + f(\phi_1; \phi_2 - \phi_3, 0) - f(0; \phi_1, \phi_2 - \phi_3), \\ \dot{\phi}_2 &= \Delta_{24} + f(\phi_2; \phi_1 + \phi_3, 0) - f(0; \phi_1 + \phi_3, \phi_2), \\ \dot{\phi}_3 &= \Delta_{34} + f(\phi_3; \phi_1 + \phi_3, \phi_2) - f(0; \phi_1 + \phi_3, \phi_2).\end{aligned}\tag{24}$$

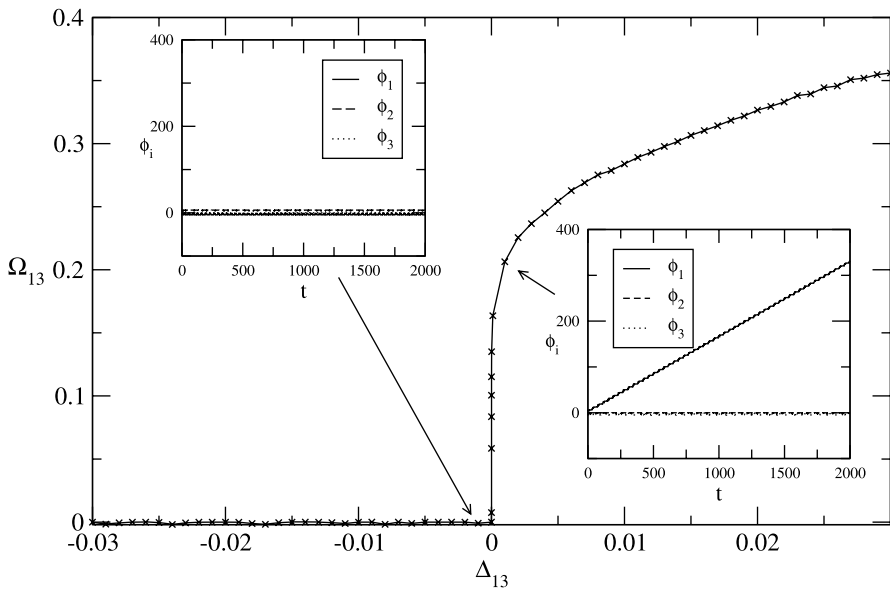


**Fig. 6** The main graph shows the frequency difference  $\Omega_{13}$  for (4) with parameters (21) as a function of detuning  $\Delta_{13}$  between the first and third oscillator for  $\Delta_{24} = \Delta_{34} = 0$ . Note that oscillators remain frequency synchronized for  $\Delta_{13} \leq 0$  but quickly break synchrony for  $\Delta_{13} > 0$ ; this is evidence of the attractor being a heteroclinic ratchet. The insets show time evolution of the phase differences  $\phi_i$  for a positive and a negative value of  $\Delta_{13}$ ; observe that oscillators 1 and 3 are phase and frequency synchronized for  $\Delta_{13} < 0$  but neither phase nor frequency synchronized for  $\Delta_{13} > 0$

An interesting property of heteroclinic ratchets (such as that illustrated in Fig. 4) is that the qualitative response to detuning depends on the sign of the detuning. An example showing  $\Omega_{13}$ , the difference between the observed average frequencies of the oscillators 1 and 3, as a function of  $\Delta_{13}$  is given in Fig. 6. Considering (24), one can observe that since the heteroclinic ratchet includes winding connections in the  $+\phi_1$  direction but no connections winding in the  $-\phi_1$  direction, the oscillator system responds to  $\Delta_{13} > 0$  by breaking frequency synchronization of the oscillator pair (1, 3), whereas  $\Delta_{13} \leq 0$  leaves the frequency synchronization unchanged,  $\Omega_{13} = 0$ . There is a similar response for the difference between oscillators 2 and 4 as can be seen by the symmetry of the original system (4). Small positive and/or negative detunings  $\Delta_{34}$  do not have any qualitative effect on the dynamics of (24) near the heteroclinic ratchet considered, since it does not include winding connections in the  $+\phi_3$  or  $-\phi_3$  directions.

#### 4.2 Response of the System to Noise and Detuning

Here, we consider the effect of additive white noise with amplitude  $\varepsilon$  for the system (24) with  $\Delta_{34} = 0$  and  $\Delta_{13} = \Delta_{24} = \Delta$ . Recall that the heteroclinic cycle shown in Fig. 4b contains two nonwinding and two winding trajectories, and in the ideal case (no noise and no detuning) a solution converging to the heteroclinic ratchet oscillates near the nonwinding trajectories. However, addition of noise to the system without



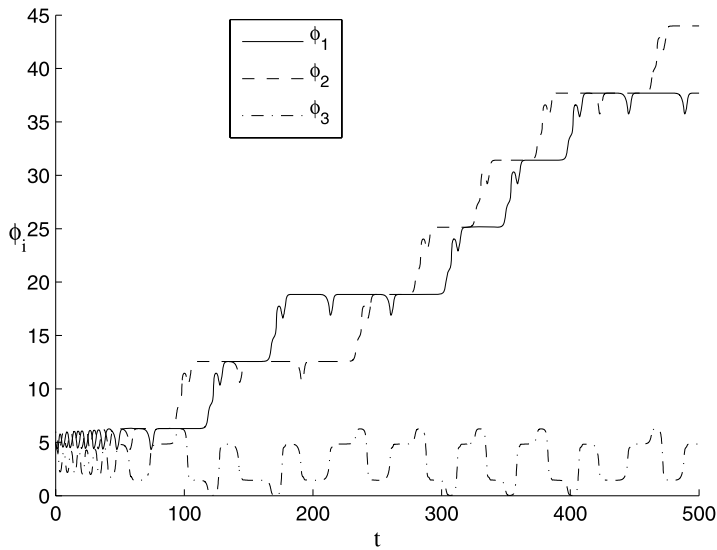


**Fig. 7** A solution of the system (19) with no detuning and additive white noise (amplitude =  $10^{-6}$ ) for the parameter set (21). Noise causes the system to have repeated phase slips in the  $+\phi_1$  and  $+\phi_2$  directions

detuning will cause phase slips in  $+\phi_1$  and  $+\phi_2$  directions such that winding will be present even for arbitrary low amplitude  $\varepsilon$  (see Fig. 7).

We define the winding frequency of the system (4) as  $\Omega = (\Omega_{13} + \Omega_{24})/(2\pi)$  and the corresponding winding period as  $T = \Omega^{-1}$ . For a given noise amplitude  $\varepsilon$  and detuning  $\Delta$ , the winding frequency  $\Omega(\varepsilon, \Delta)$  can be obtained numerically as in Fig. 9. Even in the presence of negative detuning  $\Delta < 0$ , arbitrarily low amplitude noise will eventually cause fluctuations such that the winding trajectories in the ratchet are visited. This can be seen from Fig. 9a, where  $\Omega$  is plotted as a function of  $\Delta < 0$  for different noise amplitudes  $\varepsilon$ .

The effect of noise on the dynamics near the heteroclinic ratchet is different when  $\Delta > 0$  is considered. In this case noise can cause fluctuations such that nonwinding trajectories are visited more frequently than in the case of positive detuning without noise. This happens only when  $0 < \Delta \ll \varepsilon$  and diminishes the observed winding frequency  $\Omega$ .

Note that the winding period  $T$  in the absence of noise varies linearly with  $\log(\Delta)$  for  $0 < \Delta \ll 1$  (see Fig. 9c). It is because  $T$  can be expressed in terms of  $\Delta$  as

$$T(0, \Delta) = \Omega(0, \Delta) \cong -\frac{1}{\lambda} \ln(\Delta) = -\frac{\ln(10)}{\lambda} \log(\Delta),$$

as expected from the residence time near an equilibrium of a perturbed homoclinic cycle (Stone and Holmes 1990), where  $\lambda$  is the most positive eigenvalue at the saddle and  $\log = \log_{10}$ . In our case,  $\lambda = 0.74$  as found in Sect. 3, and the corresponding slope of line representing the relation between  $T$  and  $\log(\Delta)$  is  $-\ln(10)/\lambda = -3.11$ , consistent with simulations (see Fig. 9c).

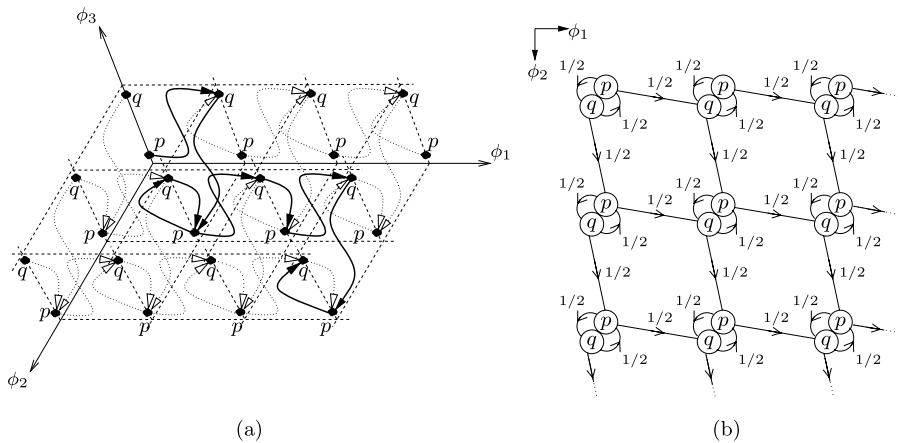


**Fig. 8** Schematic diagrams demonstrating trajectories switching between saddles of the heteroclinic ratchet in Fig. 4b under small additive noise. **(a)** A trajectory switching randomly between saddles  $p$  and  $q$  is shown on the lift of  $\mathbb{T}^3$  to  $\mathbb{R}^3$ . **(b)** All possible switchings between saddles  $p$  and  $q$  with probabilities under homogeneous noise are plotted as projected onto  $\phi_1$ - $\phi_2$  plane

In the absence of detuning, the winding period depends on the noise amplitude in a similar way but with a multiplier 2, that is,  $T(\varepsilon, 0) = 2T(0, \varepsilon)$ . In order to see this, recall that the heteroclinic ratchet contains one winding trajectory and one nonwinding trajectory from  $p$  to  $q$  (or from  $q$  to  $p$ ) (see Fig. 4b). Since a solution converging to a heteroclinic network spends most of its time near equilibria, we can consider the effect of weak noise as perturbations near the equilibria. Considering the lower (upper) equilibrium  $p$  ( $q$ ), nonwinding and winding trajectories are chosen with equal probabilities in the case of the unbiased homogeneous noise as a result of the presence of invariant subspace  $V_3^2$  ( $V_3^1$ ). A typical trajectory switching randomly between the saddles of the heteroclinic ratchet under weak noise is illustrated in Fig. 8a on the lift of  $\mathbb{T}^3$  to  $\mathbb{R}^3$ , and all possible winding and nonwinding switchings for trajectories are shown in Fig. 8b where each switching has the same probability 0.5. Therefore, on average, a trajectory in one winding period visits both equilibria  $p$  and  $q$ . Thus, the winding period is twice as large as the winding period for  $\varepsilon = 0$  and  $\Delta > 0$  where the trajectories pass one equilibria in each winding period as only the winding trajectories of the ratchet are visited. The consequence of this can also be seen in Fig. 9b, where  $\Omega(\varepsilon, \Delta) \cong \Omega(0, \varepsilon)/2$  for  $0 < \Delta \ll \varepsilon$ .

### 4.3 Frequency Synchronization Without Phase Synchronization

Adding unbiased homogeneous noise (without detuning) can lead to frequency synchronization *without* phase synchronization; one can have a situation where  $\phi_1$  and  $\phi_2$  are frequency synchronized but  $\phi_1 - \phi_2$  is unbounded. This occurs because the presence of unbiased noise means that the average frequency of the phase slips in the  $+\phi_1$  and  $+\phi_2$  directions should be equal, that is,  $\lim_{t \rightarrow \infty} \frac{\phi_1 - \phi_2}{t} = 0$ .

Using the usual phase variables, we can write this as

$$\lim_{t \rightarrow \infty} \frac{\theta_1 - \theta_3 - \theta_2 + \theta_4}{t} = 0. \quad (25)$$

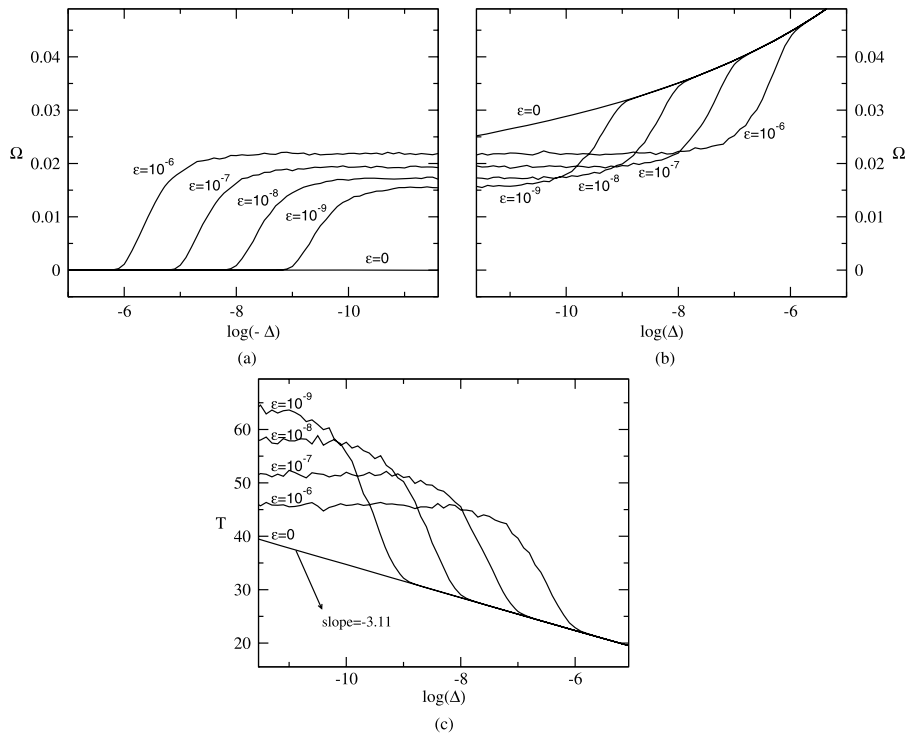


**Fig. 9** Winding frequency  $\Omega$  plotted against  $\log(\Delta)$  for (a)  $\Delta < 0$ , (b)  $\Delta > 0$  and additive noise of amplitude  $\varepsilon$ . The corresponding winding period  $T = \Omega^{-1}$  is plotted in (c) for  $\Delta > 0$ . Note that for  $|\Delta| \ll \varepsilon$ , noise dominates causing a  $\Delta$ -independent winding, while  $\Delta > \varepsilon$  implies winding and  $\Delta < -\varepsilon$  gives no winding. The winding period  $T$  varies linearly with  $\log(\Delta)$  until noise effects dominate

Due to the symmetry of the system when the detunings are zero, we have  $\Omega_{34} = \lim_{t \rightarrow \infty} \frac{\phi_3}{t} = \lim_{t \rightarrow \infty} \frac{\theta_3 - \theta_4}{t} = 0$ . Thus, (25) implies  $\Omega_{12} = \lim_{t \rightarrow \infty} \frac{\theta_1 - \theta_2}{t} = 0$ . As a result, the oscillator pairs (1, 2) and (3, 4) are frequency synchronized.

On the other hand, arbitrary small homogeneous noise will cause all oscillator pairs to lose phase synchronization. Moreover, the oscillator pairs (1, 3) and (2, 4) lose their frequency synchronization since noise results in repeated forward phase slips of the oscillators 1 and 2 due to the winding connections of the ratchet, whereas the pairs (1, 2) and (3, 4) maintain their frequency synchronization without phase synchronization.

#### 4.4 Heteroclinic Ratchets in a System Without Symmetry

Although the system (4) has  $S_2$  permutation and  $\mathbb{T}^1$  phase-shift symmetries, we show in this section that these symmetries are not necessary for the existence of a heteroclinic ratchet. In fact, for the system (4), the  $S_2$  symmetry merely simplifies the existence and stability discussions in Sects. 3.1 and 3.2 and gives rise to a clear explanation for the emergence of the heteroclinic ratchet via the synchrony-breaking bifurcation in Theorem 1. On the other hand,  $\mathbb{T}^1$  symmetry makes it possible to describe

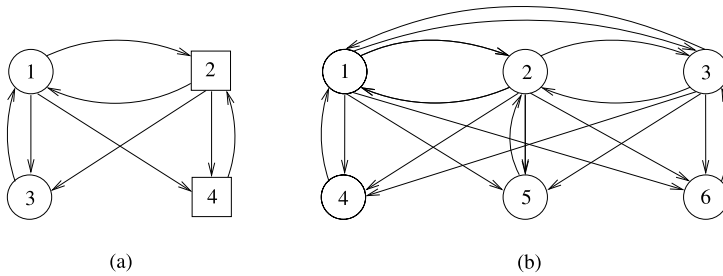


**Fig. 10** Two coupled cell networks that allow heteroclinic ratchets. **(a)** A 4-cell network with the same coupling structure as in Fig. 1 but with two different cell types. This network has no permutation symmetry. **(b)** A 6-cell network with identical cells

heteroclinic connections between periodic orbits of (4) by heteroclinic connections between saddle equilibria of (8) with the help of the phase-difference reduction.

In order to see that  $S_2$  and  $\mathbb{T}^1$  symmetries are not necessary for the existence of heteroclinic ratchets, we consider a perturbed system of (4) on  $\mathbb{T}^4$ :

$$\begin{aligned}\dot{\theta}_1 &= \omega + f(\theta_1; \theta_2, \theta_3) + \alpha_1 \cos(\theta_1), \\ \dot{\theta}_2 &= \omega + f(\theta_2; \theta_1, \theta_4) + \alpha_2 \cos(\theta_2), \\ \dot{\theta}_3 &= \omega + f(\theta_3; \theta_1, \theta_2) + \alpha_1 \cos(\theta_3), \\ \dot{\theta}_4 &= \omega + f(\theta_4; \theta_1, \theta_2) + \alpha_2 \cos(\theta_4).\end{aligned}\tag{26}$$

Note that the above system has the same coupling structure as in Fig. 1, but with two different cell types, namely the cells 1 and 3 are of one type, and the cells 2 and 4 are of another type as illustrated in Fig. 10a. This is due to the  $\alpha_j \cos(\theta_k)$  terms in (26). The balanced coloring method from Sect. 2.1 only gives three nontrivial invariant subspaces  $V_2$ ,  $V_3^1$ , and  $V_3^2$ , since in the case of different cell types, only cells of the same type can have the same color. Note that these invariant subspaces are the ones that contain the saddles and the connections of the heteroclinic ratchet for the symmetric system (4). Therefore, we expect robustness of the heteroclinic ratchet for (26) that exists when  $\alpha_1 = \alpha_2 = 0$ . Here, by robustness we mean persistence under small enough perturbations that preserve the connection structure and cell types, including perturbations of the parameters  $\alpha_1$  and  $\alpha_2$ . We denote by  $\bar{p}(0)$  and  $\bar{q}(0)$  the saddle periodic orbits of (26) in  $V_2$  for  $\alpha_1 = \alpha_2 = 0$  corresponding to the saddle equilibria  $p$  and  $q$  in Fig. 4 for the phase-difference system (8). In  $\mathbb{T}^4$ , the heteroclinic ratchet is between the saddle periodic orbits  $\bar{p}(0)$  and  $\bar{q}(0)$ , whereas the connections between these are the two-dimensional unstable manifolds of  $\bar{p}(0)$  and  $\bar{q}(0)$ , which are contained in  $V_3^1$  and  $V_3^2$ , respectively. Similar to the case in the phase-difference system,  $\bar{p}(0)$  ( $\bar{q}(0)$ ) is a sink in  $V_3^2$  ( $V_3^1$ ) and a saddle in  $V_3^1$  ( $V_3^2$ ). By robustness, we expect the heteroclinic ratchet in  $\mathbb{T}^4$  between the perturbed periodic orbits  $\bar{p}(\alpha)$  and  $\bar{q}(\alpha)$  to persist for small enough  $\alpha_1$  and  $\alpha_2$ . In Fig. 11, a solution of the perturbed system with additive white noise is shown for  $\alpha_1 = 0.01$  and  $\alpha_2 = 0.02$ . Repeated forward phase slips of the oscillators 1 and 2 are indicators of the presence of a hete-

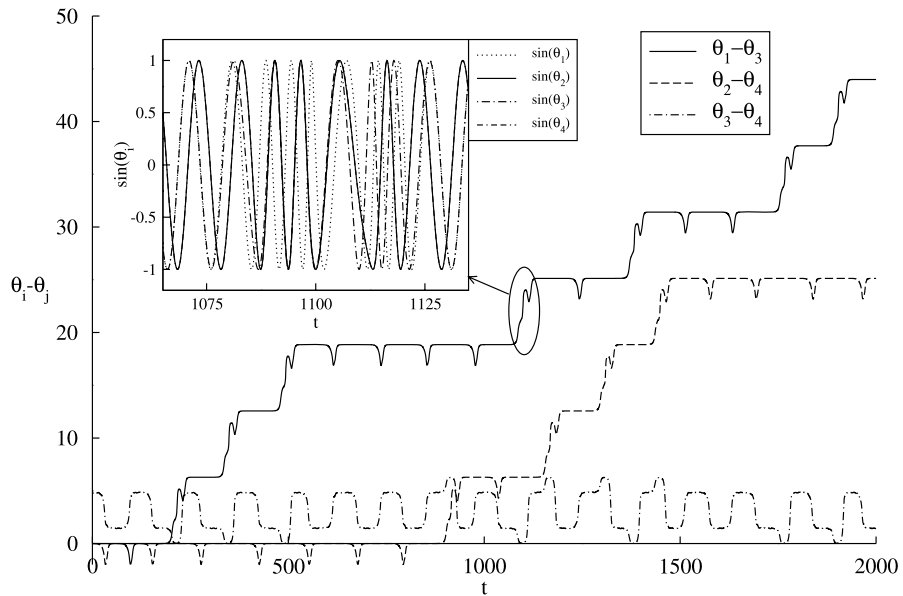


**Fig. 11** A solution of the system (26) with additive white noise (amplitude =  $10^{-6}$ ) for  $\alpha_1 = 0.01$  and  $\alpha_2 = 0.02$ . Repeated phase slips in specific directions indicate the presence of an attracting heteroclinic ratchet. The inset shows the oscillations in detail when the first oscillator undergoes a forward phase slip relative to the others

roclinic ratchet. The inset in this figure shows clearly the transition from one periodic orbit to another as discussed above, accompanied by a forward phase slip of oscillator 1 relative to the other oscillators.

#### 4.5 Heteroclinic Ratchets in Larger Coupled Oscillator Network

One may expect to observe heteroclinic ratchets in larger oscillator networks. However, due to the growth in phase space dimension, analysis of heteroclinic ratchets can be quite complex as these may include unstable manifolds of saddles with dimension greater than one. Here, we consider the 6-cell network illustrated in Fig. 10b and simulate the same coupled oscillator dynamics in (1) where  $N = 6$ ,  $c_{ij}$ 's are determined by the given network structure, and the coupling function  $g$  is the same as in (20). Similar to the example in Sect. 3, ratcheting solutions are found when small additive noise is applied. The phase differences are illustrated in Fig. 12, which suggests the existence of an attracting heteroclinic ratchet in  $\mathbb{T}^6$ .

The network structure given in Fig. 10b can be generalized to  $2N$ -cell networks to give heteroclinic ratchets in larger-dimensional tori. To analyze the structure of heteroclinic ratchets in  $\mathbb{T}^N$  and to find conditions for networks that allow heteroclinic ratchets are interesting topics motivated by this work.

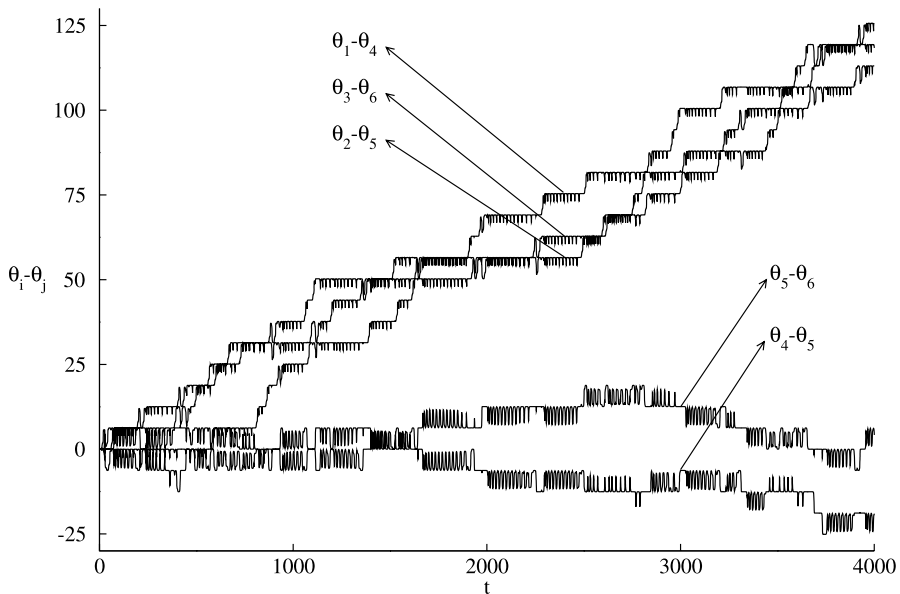


**Fig. 12** A solution of the coupled oscillator network in Fig. 10b under small additive white noise (amplitude =  $10^{-4}$ ) with zero initial states. The equations for the dynamics are as in (1), (20), and the parameters are  $\alpha_1 = 1.15$ ,  $r_2 = 0.3$ , and  $r_3 = -0.1$ . The phase differences between certain pairs of oscillators increase monotonically which suggest the existence of an attracting heteroclinic ratchet including connections winding in  $\theta_1 - \theta_4$ ,  $\theta_2 - \theta_5$ , and  $\theta_3 - \theta_6$  directions

#### 4.6 Other Comments

As the existence and robustness of heteroclinic ratchets rely only on the presence of invariant subspaces and the existence of winding heteroclinic connections, we believe that heteroclinic ratchets will be present in a variety of coupled dynamical systems. Moreover, they will not occur in purely symmetry-forced heteroclinic networks because these will have unstable manifold branches that are symmetrically related.

The four-cell example we have discussed here is interesting in that we believe that it is in some sense the simplest; for example, robust heteroclinic attractors cannot occur in fewer than four globally coupled oscillators. In applications, one can think of the network as a possible dynamical *motif* (Zhigulin 2004), i.e., a dynamical building block for a network with a more complex function. Motifs in networks have been investigated in different areas since the work of Milo et al. (2002), and asymmetrically coupled small networks are found to exist in neural networks as functional motifs (Sporns and Kötter 2004).

The analysis of the present system in the presence of detuning shows that *extreme sensitivity to detuning* (Ashwin et al. 2006) may be a subtle phenomenon with, for example, rectification properties, and we conjecture that such dynamical functions may be of use for information processing, for example, in neural systems.

There remain a number of questions and details to be investigated for the example presented here; for instance, understanding the detailed dynamics on adding nonzero

detuning will be quite a challenge, as will be obtaining a full understanding of the bifurcation structure.

**Acknowledgements** We thank Mike Field for discussions relating to this work and Nikita Agarwal for her corrections. We also would like to thank the anonymous reviewers, whose comments improved the quality of the paper.

## Appendix: Instability of the Heteroclinic Ratchet for $r_k = 0$ , $k = 3, 4, \dots$

In Sect. 3, it is shown that for the system (19), an asymptotically stable heteroclinic ratchet exists that connects the equilibria  $p$  and  $q$ . Here, we show that this heteroclinic ratchet cannot be asymptotically stable if only the first two harmonics of the coupling function are considered. That is,

$$g(x) = -\sin(x + \alpha_1) + r_2 \sin(2x + \alpha_2). \quad (27)$$

The equilibria  $p = (0, 0, p_3)$  and  $q = (0, 0, 2\pi - p_3)$  in  $V_2$  are given by

$$p_3 = \cos^{-1} \left( \frac{\cos \alpha_1}{2r_2 \cos \alpha_2} \right). \quad (28)$$

This can be obtained from (19) by setting  $\phi_1 = \phi_2 = \dot{\phi}_3 = 0$ . Let us calculate the eigenvalues at  $p$ . Linearizing (19) at  $p$  gives

$$\lambda^\mp(p) = g'(\mp p) + 2g'(0), \quad \lambda^0 = g'(p) + g'(-p), \quad (29)$$

where  $\lambda^+(p)$  and  $\lambda^-(p)$  correspond to the eigenvectors in  $V_3^1 \setminus V_2$  and  $V_3^2 \setminus V_2$ , respectively, and  $\lambda^0(p)$  is the eigenvalue corresponding to the eigenvector in  $V_2 = V_3^1 \cap V_3^2$ .

Without loss of generality, we assume that the heteroclinic network connects the equilibrium  $p$  to its symmetric image  $q = \rho(p)$  on  $V_3^1$  and  $q$  to  $p$  on  $V_3^2$ . Then, for the asymptotic stability of the heteroclinic network, the following conditions are necessary:

$$\text{Existence of saddles } p \text{ and } q \text{ (from (28))}: \quad \left| \frac{\cos \alpha_1}{2r_2 \cos \alpha_2} \right| < 1. \quad (30)$$

$$\text{Existence of connections on } V_3^1: \quad \lambda^0(p) = g'(p) + g'(-p) < 0, \quad (31)$$

$$\lambda^+(p) > 0, \quad \lambda^-(p) < 0. \quad (32)$$

$$\text{Asymptotic stability condition (Melbourne 1989)}: \quad \left| \frac{\lambda^+(p)}{\lambda^-(p)} \right| < 1. \quad (33)$$

Equations (32) and (33) imply

$$\lambda^+(p) + \lambda^-(p) = g'(p) + g'(-p) + 4g'(0) < 0. \quad (34)$$

We first assume that  $r_2 \cos \alpha_2 < 0$ . From (31) we have

$$-2 \cos p \cos \alpha_1 + 4r_2 \cos 2p \cos \alpha_2 < 0, \quad (35)$$

$$-2 \cos p \cos \alpha_1 + 8r_2 \cos^2 p \cos \alpha_2 - 4r_2 \cos \alpha_2 < 0. \quad (36)$$

Substituting (28), we get

$$\frac{\cos^2 \alpha_1}{r_2 \cos \alpha_2} - 4r_2 \cos \alpha_2 < 0.$$

Our assumption then implies that

$$\frac{\cos^2 \alpha_1}{4r_2^2 \cos^2 \alpha_2} > 1,$$

which contradicts (30). On the other hand, if we assume that  $r_2 \cos \alpha_2 > 0$ , the condition (34) cannot be satisfied since

$$\begin{aligned} \lambda^+(p) + \lambda^-(p) &= g'(p) + g'(-p) + 4g'(0) \\ &= -2 \cos p \cos \alpha_1 + 8r_2 \cos^2 p \cos \alpha_2 - 4r_2 \cos \alpha_2 \\ &\quad - 4 \cos \alpha_1 + 8r_2 \cos \alpha_2, \end{aligned}$$

and substituting (28), one gets

$$\begin{aligned} \lambda^+(p) + \lambda^-(p) &= -\frac{\cos^2 \alpha_1}{r_2 \cos \alpha_2} + \frac{2 \cos^2 \alpha_1}{r_2 \cos \alpha_2} + 4r_2 \cos \alpha_2 - 4 \cos \alpha_1 \\ &= \left( \frac{\cos \alpha_1}{\sqrt{r_2 \cos \alpha_2}} - 2\sqrt{r_2 \cos \alpha_2} \right)^2 \geq 0. \end{aligned}$$

Thus, (34) is not satisfied.

## References

- Aguiar, M.A.D., Dias, A.P.S., Golubitsky, M., Leite, M.C.A.: Homogenous coupled cell networks with  $S_3$ -symmetric quotient. DCDS Supplement, pp. 1–9 (2007)
- Aguiar, M.A.D., Ashwin, P., Dias, A.P.S., Field, M.: Robust heteroclinic cycles in coupled cell systems: identical cells with asymmetric inputs. Preprint (2009)
- Ashwin, P., Borresen, J.: Encoding via conjugate symmetries of slow oscillations for globally coupled oscillators. Phys. Rev. E **70**(2), 026203 (2004)
- Ashwin, P., Borresen, J.: Discrete computation using a perturbed heteroclinic network. Phys. Lett. A **347**(4–6), 208–214 (2005)
- Ashwin, P., Swift, J.W.: The dynamics of  $n$  weakly coupled identical oscillators. J. Nonlinear Sci. **2**(1), 69–108 (1992)
- Ashwin, P., Burylko, O., Maistrenko, Y., Popovych, O.: Extreme sensitivity to detuning for globally coupled phase oscillators. Phys. Rev. Lett. **96**(5), 054102 (2006)
- Ashwin, P., Orosz, G., Wordsworth, J., Townley, S.: Dynamics on networks of clustered states for globally coupled phase oscillators. SIAM J. Appl. Dyn. Syst. **6**(4), 728–758 (2007)



- Ashwin, P., Burylko, O., Maistrenko, Y.: Bifurcation to heteroclinic cycles and sensitivity in three and four coupled phase oscillators. *Physica D* **237**, 454–466 (2008)
- Busse, F.H., Clever, R.M.: Nonstationary convection in a rotating system. In: Müller, U., Roesner, K.G., Schmidt, B. (eds.) *Recent Developments in Theoretical and Experimental Fluid Dynamics*, pp. 376–385. Springer, Berlin (1979)
- Ermentrout, G.B.: *A Guide to XPPAUT for Researchers and Students*. SIAM, Pittsburgh (2002)
- Feng, B.Y., Hu, R.: A survey on homoclinic and heteroclinic orbits. *Appl. Math. E-Notes* **3**, 16–37 (2003) (electronic)
- Golubitsky, M., Stewart, I.: *The Symmetry Perspective*. Birkhäuser, Basel (2002)
- Golubitsky, M., Stewart, I.: Nonlinear dynamics of networks: The groupoid formalism. *Bull. Am. Math. Soc. (N.S.)* **43**(3), 305–364 (2006) (electronic)
- Golubitsky, M., Pivato, M., Stewart, I.: Interior symmetry and local bifurcation in coupled cell networks. *Dyn. Syst.* **19**(4), 389–407 (2004)
- Guckenheimer, J., Holmes, P.: Structurally stable heteroclinic cycles. *Math. Proc. Camb. Philos. Soc.* **103**, 189–192 (1988)
- Hansel, D., Mato, G., Meunier, C.: Clustering and slow switching in globally coupled phase oscillators. *Phys. Rev. E* **48**(5), 3470–3477 (1993)
- Hofbauer, J., Sigmund, K.: *Evolutionary Games and Population Dynamics*. Cambridge University Press, Cambridge (1998)
- Kiss, I.Z., Rusin, C.G., Kori, H., Hudson, J.L.: Engineering complex dynamical structures: Sequential patterns and desynchronization. *Science* **316**, 1886–1889 (2007)
- Kori, H., Kuramoto, Y.: Slow switching in globally coupled oscillators: Robustness and occurrence through delayed coupling. *Phys. Rev. E* **63**, 046214 (2001)
- Krupa, M.: Robust heteroclinic cycles. *J. Nonlinear Sci.* **7**(2), 129–176 (1997)
- Krupa, M., Melbourne, I.: Asymptotic stability of heteroclinic cycles in systems with symmetry. *Ergod. Theory. Dyn. Syst.* **15**, 121–147 (1995)
- Kuramoto, Y.: *Chemical Oscillations, Waves and Turbulence*. Springer, Berlin (1984)
- Melbourne, I.: Intermittency as a codimension-three phenomenon. *J. Dyn. Differ. Equ.* **1**(4), 347–367 (1989)
- Milnor, J.: On the concept of attractor. *Commun. Math. Phys.* **99**, 177–195 (1985)
- Milo, R., Shen-Orr, S., Itzkovitz, S., Kashtan, N., Chklovskii, D., Alon, U.: Network motifs: Simple building blocks of complex networks. *Science* **298**, 824–827 (2002)
- Rabinovich, M.I., Huerta, R., Varona, P., Afraimovich, V.S.: Generation and reshaping of sequences in neural systems. *Biol. Cybern.* **95**, 519–536 (2006a)
- Rabinovich, M.I., Varona, P., Selverston, A.I., Abarbanel, H.D.I.: Dynamical principles in neuroscience. *Rev. Mod. Phys.* **95**, 519–536 (2006b)
- Sakaguchi, H., Kuramoto, Y.: A soluble active rotator model showing phase transitions via mutual entrainment. *Prog. Theor. Phys.* **76**(3), 576–581 (1986)
- Sporns, O., Kötter, R.: Motifs in brain networks. *PLoS Biol.* **2**(11), 1910–1918 (2004)
- Stone, E., Holmes, P.: Random perturbations of heteroclinic attractors. *SIAM J. Appl. Math.* **50**(3), 726–743 (1990)
- Strogatz, S.H.: From Kuramoto to Crawford: Exploring the onset of synchronization in populations of coupled oscillators. *Physica D* **143**, 1–20 (2000)
- Zhai, Y.M., Kiss, I.Z., Daido, H., Hudson, J.L.: Extracting order parameters from global measurements with application to coupled electrochemical oscillators. *Physica D* **205**, 57–69 (2005)
- Zhigulin, P.Z.: Dynamical motifs: Building blocks of complex dynamics in sparsely connected random networks. *Phys. Rev. Lett.* **92**(23), 238701 (2004)